second- and third-row transition metals, localization of electrons in both discrete metal and semiquinone orbitals is seldom seen due to the larger energy separation between ligand and metal orbitals. As a result, electrons pair in the lowest energy orbitals with any remaining unpaired electrons being localized either on the metal, as in $Re^{VI}(3,5\text{-}DBCat)_3$,[8] or on the ligand, as in $Re_2(CO)_7(PhenSQ)_2$.[12] Coordination of quinones to divalent rhenium has not previously been observed, and all mononuclear complexes of the metal in this oxidation state are paramagnetic with metal-localized radicals. However, a different behavior is observed in the divalent rhenium compound $Re(CO)_3(C_{14}H_{21}NO)(C_{28}H_{39}NO_2)$. Structural features of the iminophenolate ligand clearly show radical localization within the carbonyl region of this ligand, and strong antiferromagnetic coupling to the unpaired electron on rhenium results in a paramagnetic complex with radical localization on the phenoxazinyl ligand. EPR spectral data on the compound corroborate well with this charge distribution, definitively showing radical localization on the phenoxazinyl ligand.

Monodentate coordination of the iminophenolate ligand is also unique. Previous crystallographic characterization of Fe(saloph)CatH showed similar monodentate coordination of a catecholate ligand.[9c] The saloph ligand in this iron(III) complex occupied the four basal positions of a square pyramid and prevented chelation of catechol. In the rhenium complex, three carbonyl ligands occupy facial positions and the iminophenolate ligand could chelate upon cleavage of one carbonyl ligand. However, all attempts to induce further carbonyl cleavage, either by photolysis or reaction with trimethylamine *N*-oxide, were unsuccessful, and no bidentate coordination of the iminophenolate ligand was observed.

Formation of both radical ligands in the title compound clearly involves Schiff-base condensation reactions of 3,5-di-*tert*-butylsemiquinone and ammonia. These reactions were also proposed for formation of the biquinone Cat-N-BQ ligand (see Scheme I), and Girgis suggested that due to steric constraints only the 2,4-di-*tert*-butyl-iminoquinone isomer would be formed in the initial condensation reaction.[4b] However, complexation of 3,5-di-*tert*-butyliminophenolate to rhenium in $Re(CO)_3(C_{14}H_{21}NO)(C_{28}H_{39}NO_2)$ is evidence that both iminoquinone isomers are formed in these initial reactions. Steric constraints would have an effect on further reactions of the iminoquinones involved in formation of Cat-N-BQ ligands with only the 2,4-substituted isomer having the correct conformation to react through further Schiff-base condensation with 3,5-di-*tert*-butylcatechol. 3,5-Di-*tert*-butyliminoquinone is likely a side product in reactions giving $M^{II}(Cat\text{-}N\text{-}BQ)_2$ complexes, but in reactions with $Re(CO)_5Br$, this ligand reacts further with rhenium to give the isolated product.

Formation of 1-hydroxy-2,4,6,8-tetra-*tert*-butylphenoxazinylate radicals are known to occur through additional reactions of Cat-N-BQ anions in basic media.[13] These reactions were not previously outlined but likely involve initial addition of the oxygen on one quinone ring to the carbon positioned ortho to the imine functionality on the other ring, followed by deprotonation and oxidation in air. Coordination of this radical to a variety of organometallic fragments, including $Re(CO)_4$, has previously been studied by EPR spectroscopy, and chelation to metals through the deprotonated hydroxy oxygen atom and the nitrogen atom was proposed.[10] Crystallographic characterization of $Re(CO)_3(C_{14}H_{21}NO)(C_{28}H_{39}NO_2)$ is the first structural characterization of this ligand and confirms bidentate coordination to metals.

Acknowledgment. This research was supported by the National Science Foundation under Grants CHE 85-03222, CHE 88-09923, and CHE 84-12182 (X-ray instrumentation).

Supplementary Material Available: Tables containing details of the structure determination and refinement, anisotropic thermal parameters, and a complete list of bond distances and angles for $Re(CO)_3(C_{14}H_{21}NO)(C_{28}H_{39}NO_2)$ (12 pages); a listing of observed and calculated structure factors (23 pages). Ordering information is given on any masthead page.

Contribution from the Department of Chemistry, Northwestern University, Evanston, Illinois 60208

Mixed-Metal Selenides: Synthesis and Characterization of the $Ni(Se_2)(WSe_4)^{2-}$ and $M(WSe_4)_2^{2-}$ (M = Ni, Pd) Anions

Mohammad A. Ansari, Chung-Nin Chau, Charles H. Mahler, and James A. Ibers*

Received June 24, 1988

Reaction of $[NH_4]_2[WSe_4]$ dissolved in DMF with a suspension of $Ni(acac)_2$ in DMF in the presence of $[PPh_4]Cl$ affords $[PPh_4]_2[Ni(Se_2)(WSe_4)]$. A similar reaction involving $NiCl_2(PPh_3)_2$ in place of $Ni(acac)_2$ affords $[PPh_4]_2[Ni(WSe_4)_2]$, while the use of $PdCl_2(C_6H_5CN)_2$ affords $[PPh_4]_2[Pd(WSe_4)_2]$. The $Ni(Se_2)(WSe_4)^{2-}$ ion shows ^{77}Se NMR resonances at δ 1399, 855, and 608 ppm expected for the structure found in the solid state consisting of a square-planar Ni center bound to a side-on Se_2 group and to a nearly tetrahedral WSe_4 group ($[PPh_4]_2[Ni(Se_2)(WSe_4)]$, $Z = 4$, $P2_1/n$, $a = 14.222$ (6) Å, $b = 17.168$ (7) Å, $c = 19.976$ (8) Å, $\beta = 110.3$ (2)°, $R(F^2) = 0.076$ for 9932 observations). This ion has no known sulfide analogue. The $M(WSe_4)_2^{2-}$ ions (M = Ni, Pd) are closely analogous to the known $Ni(WS_4)_2^{2-}$ ion and show two ^{77}Se NMR resonances (Ni 1628, 994 ppm; Pd 1673, 1135 ppm) consistent with the structure found in the solid state for $[PPh_4]_2[Ni(WSe_4)_2]$ in which the square-planar Ni center is bound to two nearly tetrahedral WSe_4 centers ($Z = 1$, $P\bar{1}$, $a = 9.347$ (3) Å, $b = 12.410$ (3) Å, $c = 12.557$ (3) Å, $\alpha = 65.76$ (1)°, $\beta = 84.61$ (2)°, $\gamma = 69.83$ (2)°, $R(F^2) = 0.090$ for 7295 observations). While the $Pd(WSe_4)_2^{2-}$ ion is stable in DMF solution at room temperature, the corresponding $Ni(WSe_4)_2^{2-}$ ion decomposes to form the $Ni(Se_2)(WSe_4)^{2-}$ ion.

Introduction

Soluble metal sulfides[1-3] and mixed-metal sulfides[4-6] continue to be of interest. Among mixed-metal sulfides, M-Fe-S systems (M = Mo, W) have attracted the most attention because of their relevance to the nitrogenase problem.[7,8] The ligating behavior of MS_4^{2-} toward M′ to form $M'(MS_4)_2^{2-}$ (M = Mo, W; M′ = Fe, Co, Ni, Pd, Pt, Zn, Cd, Hg) has been studied in detail.[1,9] Some other heteropolythiometalates, e.g., $FeX_2(MS_4)^{2-}$ (X = Cl, PhS), have also been reported.[10,11] The corresponding selenium

(1) Müller, A.; Diemann, E.; Jostes, R.; Bögge, H. *Angew. Chem., Int. Ed. Engl.* **1981**, *20*, 934-955.
(2) Müller, A. *Polyhedron* **1986**, *5*, 323-340.
(3) Draganjac, M.; Rauchfuss, T. B. *Angew. Chem., Int. Ed. Engl.* **1985**, *24*, 742-757.
(4) Averill, B. A. *Struct. Bonding (Berlin)* **1983**, *53*, 59-103.
(5) Coucouvanis, D.; Baenziger, N. C.; Simhon, E. D.; Stremple, P.; Swenson, D.; Kostikas, A.; Simopoulos, A.; Petrouleas, V.; Papaefthymiou, V. *J. Am. Chem. Soc.* **1980**, *102*, 1730-1732.
(6) McDonald, J. W.; Friesen, G. D.; Newton, W. E. *Inorg. Chim. Acta* **1980**, *46*, L79-80.
(7) Hughes, M. N., Ed. *The Inorganic Chemistry of Biological Process*; Wiley: New York, 1984.
(8) Spiro, T. G., Ed. *Molybdenum Enzymes*; Wiley-Interscience: New York, 1986.
(9) Callahan, K. P.; Piliero, P. A. *Inorg. Chem.* **1980**, *19*, 2619-2626.
(10) Coucouvanis, D.; Simhon, E. D.; Swenson, D.; Baenziger, N. C. *J. Chem. Soc., Chem. Commun.* **1979**, 361-362.

0020-1669/89/1328-0650$01.50/0

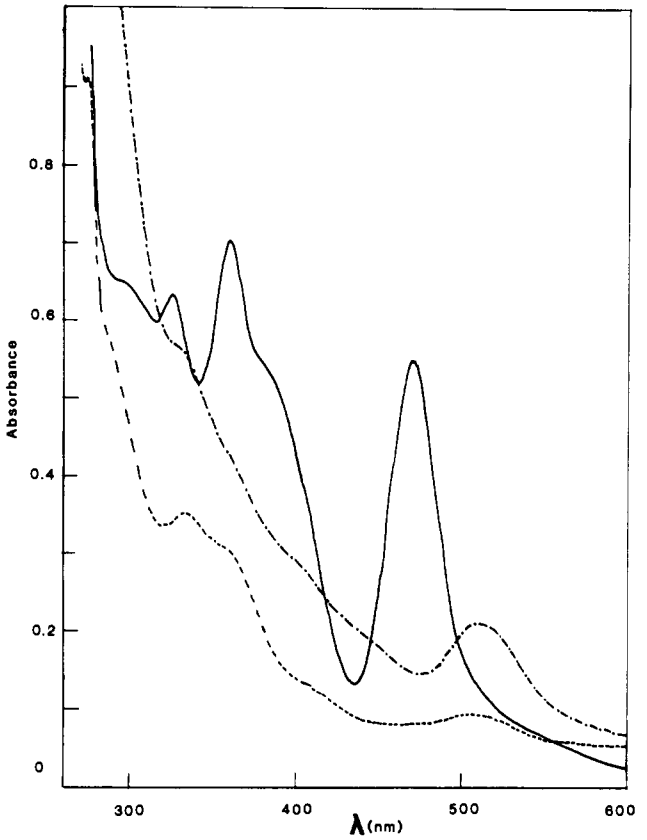

Figure 1. Electronic absorption (UV–vis) spectra: (a) $[PPh_4]_2[Ni(Se_2)(WSe_4)]$, 5×10^{-5} M, shown as ---; (b) $[PPh_4]_2[Ni(WSe_4)_2]$, 5×10^{-5} M, shown as –·–·; (c) $[PPh_4]_2[Pd(WSe_4)_2]$, 1×10^{-4} M, shown as —.

chemistry has not been developed in a parallel manner. Although there has been progress in soluble metal selenides recently,[13-15] virtually nothing is known about soluble mixed-metal selenides. From our recent studies[12-14] we anticipated that mixed-metal selenide chemistry would differ from the known mixed-metal sulfide chemistry. Here we describe the synthesis and characterization of $Ni(Se_2)(WSe_4)^{2-}$ and $M(WSe_4)_2^{2-}$ (M = Ni, Pd); the former anion has no known sulfide analogue.

Experimental Section

All reactions were carried out under a dry dinitrogen atmosphere with the use of standard Schlenk techniques. Solvents were dried and distilled before use. $[NH_4]_2[WSe_4]$ was purchased from Alfa Products, Danver, MA. $Ni(acac)_2$ and $PdCl_2(C_6H_5CN)_2$ were supplied by Strem Chemicals, Newburyport, MA. $NiCl_2(PPh_3)_2$ was purchased from Aldrich Chemical Co., Milwaukee, WI. Microanalyses were performed by Galbraith Laboratories, Inc., Knoxville, TN.

Spectral Measurements. The IR spectra were recorded on a Perkin-Elmer 283 spectrometer as KBr pellets. Electronic spectra were obtained on a Perkin-Elmer 330 UV–vis spectrophotometer. The ^{77}Se NMR spectra of DMF solutions were recorded on a Varian XLA-400 spectrometer with use of a 10-mm tunable probe and a deuterium lock. All chemical shifts are referenced to Me_2Se at $\delta = 0$ ppm. The detailed experimental procedures are described elsewhere.[15]

$[PPh_4]_2[Ni(Se_2)(WSe_4)]$ (1). When an anhydrous suspension of $Ni(acac)_2$ (25.7 mg, 0.10 mmol) in DMF (5 mL) was anaerobically stirred with a solution of $[NH_4]_2[WSe_4]$ (107 mg, 0.20 mmol) and $[PPh_4]Cl$ (75 mg, 0.20 mmol) in DMF (5 mL) for 2 h, a dark brown solution was obtained. This solution was filtered, and diethyl ether (20 mL) was added to the filtrate. This mixture was kept overnight at 0 °C to afford $[PPh_4]_2[Ni(Se_2)(WSe_4)]$ as green-brown crystals in 80% yield. Anal. Calcd for $C_{48}H_{40}NiP_2Se_6W$: C, 41.3; H, 2.9; P, 4.4; Se, 34.0; Ni, 4.2; W, 13.2. Found: C, 38.2; H, 2.7; P, 3.9; Se, 34.0; Ni, 3.6; W, 15.2. Absorption spectrum (DMF), λ_{max}, nm (ϵ, M^{-1} cm^{-1}): 510 (5475), 472 (4755), 364 (sh), 336 (19 400) (Figure 1a). IR spectrum (KBr): 315, 305 cm^{-1}. ^{77}Se NMR spectrum (DMF): δ 1399, 855, 608 ppm.

$[PPh_4]_2[Ni(WSe_4)_2]$ (2). A mixture of $[NH_4]_2[WSe_4]$ (107 mg, 0.20 mmol) and $[PPh_4]Cl$ (75 mg, 0.20 mmol) was dissolved in DMF (5 mL) and added to a solution of $NiCl_2(PPh_3)_2$ (36.6 mg, 0.10 mmol) in DMF (5 mL). The solution was stirred for 1 h and then filtered. Diethyl ether (20 mL) was added to the filtrate. When the solution was cooled to 0 °C overnight, dark red crystals of $[PPh_4]_2[Ni(WSe_4)_2]$ were obtained in 70% yield. Anal. Calcd for $C_{48}H_{40}NiP_2Se_8W_2$: C, 33.2; H, 2.3; P, 3.6; Se, 36.4; Ni, 3.4; W, 21.1. Found: C, 33.7; H, 2.4; P, 3.8; Se, 35.5; Ni, 3.5; W, 20.4. Absorption spectrum (DMF), λ_{max}, nm (ϵ, M^{-1} cm^{-1}): 512 (10 050), 394 (sh), 332 (20 890) (Figure 1b). IR spectrum (KBr): 325, 310 cm^{-1}. ^{77}Se NMR spectrum (DMF): δ 1628, 994 ppm.

$[PPh_4]_2[Pd(WSe_4)_2]$ (3). $[NH_4]_2[WSe_4]$ (107 mg, 0.20 mmol) and $[PPh_4]Cl$ (75 mg, 0.20 mmol) were dissolved in DMF (5 mL). $PdCl_2(C_6H_5CN)_2$ (38.36 mg, 0.10 mmol) dissolved in DMF (5 mL) was added dropwise, and the solution was stirred for 1 h. The color of the solution changed from maroon to red and finally to brown. This solution was filtered, and diethyl ether (20 mL) was added to the filtrate. This mixture was cooled to 0 °C overnight to yield dark red microcrystals of $[PPh_4]_2[Pd(WSe_4)_2]$ in 62% yield. Anal. Calcd for $C_{48}H_{40}P_2PdSe_8W_2$: C, 32.3; H, 2.3; P, 3.5; Se, 35.4; Pd, 6.0; W, 20.6. Found: C, 30.6; H, 2.5; P, 3.3; Se, 35.4; Pd, 6.0; W, 19.3. Absorption spectrum (DMF), λ_{max}, nm (ϵ, M^{-1} cm^{-1}): 470 (17 330), 388 (15 970), 364 (21 750), 326 (19 040) (Figure 1c). IR spectrum (KBr): 330, 315 cm^{-1}. ^{77}Se NMR spectrum (DMF): δ 1673, 1135 ppm.

Crystallographic Studies. Crystals of $[PPh_4]_2[Ni(Se_2)(WSe_4)]$ and $[PPh_4]_2[Ni(WSe_4)_2]$ were both grown by layering diethyl ether over a DMF solution of the respective compound in an 8-mm glass tube at room temperature under an atmosphere of N_2. In each case, a suitable crystal was mounted on a glass fiber and placed in the cold stream (−150 °C) of an Enraf-Nonius CAD4 diffractometer, where the unit cell was determined from 25 automatically centered reflections. Data collection continued on the CAD4 diffractometer for $[PPh_4]_2[Ni(Se_2)(WSe_4)]$, but the $[PPh_4]_2[Ni(WSe_4)_2]$ crystal was transferred to the cold stream (−150 °C) of a Picker FACS-1 diffractometer for data collection. In both cases the intensities of six standard reflections monitored throughout data collection were found constant within intensity statistics. Some crystallographic details are given in Table I; more are provided in Table SI.[18]

Procedures standard in this laboratory[19] were employed in the solution and refinement of both structures. Heavy-atom positions were located by Patterson methods, and the remaining non-hydrogen atoms were found from successive difference electron density maps. The final cycle of full-matrix least-squares refinement was carried out on F_o^2 in each case (for $[PPh_4]_2[Ni(Se_2)(WSe_4)]$ 9932 reflections and 524 variables; for

Table I. Crystallographic Details

formula	$C_{48}H_{40}NiP_2Se_6W$	$C_{48}H_{40}NiP_2Se_8W_2$
fw	1395	1737
a, Å	14.222 (6)	9.345 (3)
b, Å	17.168 (7)	12.413 (3)
c, Å	19.976 (8)	12.554 (3)
α, deg	90	65.83 (6)
β, deg	110.03 (2)	84.68 (5)
γ, deg	90	69.88 (5)
vol, Å^3	4582	1245
Z	4	1
d_{calcd}, g cm^{-3}	2.022	2.316
space group	C_{2h}^5-$P2_1/n$	C_i^1-$P\bar{1}$
T, °C	−150	−150
λ, (Mo $K\alpha_1$), Å	0.7093	0.7093
μ, cm^{-1}	78.0	109.7
transmission coeff	0.115–0.171	0.115–0.299
$R(F_o^2)$	0.076	0.090
$R_w(F_o^2)$	0.107	0.114
$R(F_o)$ ($F_o^2 > 3\sigma(F_o^2)$)	0.054	0.048
$R_w(F_o)$ ($F_o^2 > 3\sigma(F_o^2)$)	0.057	0.062

(11) Tieckelmann, R. H.; Silvis, H. C.; Kent, T. A.; Huynh, B. H.; Waszczak, J. V.; Teo, B.-K.; Averill, B. A. *J. Am. Chem. Soc.* **1980**, *102*, 5550–5559.
(12) Strasdeit, H.; Krebs, B.; Henkel, G. *Inorg. Chim. Acta* **1984**, *89*, L11–13.
(13) Wardle, R. W. M.; Chau, C.-N.; Ibers, J. A. *J. Am. Chem. Soc.* **1987**, *109*, 1859–1860.
(14) Chau, C.-N.; Wardle, R. W. M.; Ibers, J. A. *Inorg. Chem.* **1987**, *26*, 2740–2741.
(15) Wardle, R. W. M.; Bhaduri, S.; Chau, C.-N.; Ibers, J. A. *Inorg. Chem.* **1988**, *27*, 1747–1755.
(16) Wardle, R. W. M.; Mahler, C. H.; Chau, C.-N.; Ibers, J. A. *Inorg. Chem.* **1988**, *27*, 2790–2795.
(17) O'Neal, S. C.; Kolis, J. W. *J. Am. Chem. Soc.* **1988**, *110*, 1971–1973.
(18) Supplementary material.
(19) See for example: Waters, J. M.; Ibers, J. A. *Inorg. Chem.* **1977**, *16*, 3273–3277.

Table II. Positional Parameters and B_{eq} for $[PPh_4]_2[Ni(Se_2)(WSe_4)]$

atom	x	y	z	B_{eq}, Å^2
W	0.006 835 (22)	0.359 973 (17)	0.224 418 (15)	1.744 (8)
Ni	−0.060 126 (65)	0.365 997 (54)	0.335 675 (47)	1.72 (2)
Se(1)	−0.120 709 (52)	0.283 150 (41)	0.241 059 (40)	1.89 (2)
Se(2)	0.072 496 (51)	0.436 787 (42)	0.327 735 (39)	1.92 (2)
Se(3)	0.128 528 (71)	0.282 369 (69)	0.209 733 (62)	4.87 (4)
Se(4)	−0.060 91 (10)	0.439 884 (71)	0.128 253 (56)	7.02 (4)
Se(5)	−0.179 510 (57)	0.329 250 (51)	0.383 082 (44)	2.60 (2)
Se(6)	−0.054 210 (58)	0.416 775 (47)	0.443 649 (41)	2.43 (2)
P(1)	0.447 40 (13)	0.333 66 (11)	0.451 75 (10)	1.73 (5)
P(2)	−0.465 39 (12)	0.357 10 (10)	0.102 345 (90)	1.35 (4)
C(1)	0.573 46 (49)	0.339 55 (37)	0.512 91 (37)	1.5 (2)
C(2)	0.593 21 (49)	0.378 04 (40)	0.577 38 (36)	1.6 (2)
C(3)	0.692 09 (58)	0.385 77 (49)	0.621 83 (39)	2.7 (2)
C(4)	0.769 57 (52)	0.356 51 (46)	0.602 13 (40)	2.4 (2)
C(5)	0.748 93 (51)	0.317 20 (46)	0.538 97 (41)	2.3 (2)
C(6)	0.651 85 (53)	0.308 35 (45)	0.493 59 (42)	2.3 (2)
C(7)	0.361 94 (45)	0.361 55 (40)	0.495 64 (34)	1.4 (2)
C(8)	0.337 68 (50)	0.310 02 (41)	0.541 06 (38)	1.8 (2)
C(9)	0.272 87 (54)	0.334 01 (45)	0.575 79 (38)	2.1 (2)
C(10)	0.232 98 (49)	0.408 33 (42)	0.564 93 (36)	1.7 (2)
C(11)	0.256 14 (51)	0.458 52 (41)	0.520 26 (37)	1.9 (2)
C(12)	0.320 32 (50)	0.435 76 (41)	0.485 40 (36)	1.7 (2)
C(13)	0.433 51 (51)	0.397 26 (43)	0.378 46 (36)	1.9 (2)
C(14)	0.336 08 (54)	0.407 36 (52)	0.326 78 (40)	2.7 (2)
C(15)	0.323 51 (58)	0.454 78 (59)	0.268 96 (42)	3.3 (3)
C(16)	0.403 94 (62)	0.492 72 (57)	0.260 52 (39)	3.1 (3)
C(17)	0.498 62 (61)	0.483 70 (54)	0.310 61 (45)	3.0 (3)
C(18)	0.513 89 (49)	0.436 23 (47)	0.369 20 (37)	2.1 (2)
C(19)	0.425 61 (53)	0.235 03 (48)	0.419 86 (45)	2.6 (2)
C(20)	0.378 88 (69)	0.219 36 (58)	0.346 70 (50)	4.0 (3)
C(21)	0.361 21 (83)	0.141 40 (79)	0.325 19 (68)	6.0 (5)
C(22)	0.385 04 (75)	0.082 02 (63)	0.372 31 (82)	5.8 (5)
C(23)	0.429 50 (60)	0.098 10 (53)	0.443 87 (64)	4.5 (4)
C(24)	0.451 25 (54)	0.173 83 (49)	0.468 02 (50)	3.0 (3)
C(25)	−0.409 43 (48)	0.345 98 (38)	0.034 49 (34)	1.4 (2)
C(26)	−0.446 54 (50)	0.290 76 (42)	−0.019 37 (36)	1.8 (2)
C(27)	−0.400 90 (53)	0.284 90 (42)	−0.071 92 (37)	1.9 (2)
C(28)	−0.323 75 (52)	0.333 37 (44)	−0.070 73 (38)	2.0 (2)
C(29)	−0.288 13 (55)	0.388 01 (47)	−0.017 41 (42)	2.4 (2)
C(30)	−0.329 49 (53)	0.394 37 (43)	0.035 87 (39)	2.1 (2)
C(31)	−0.446 60 (46)	0.272 29 (38)	0.158 78 (36)	1.3 (2)
C(32)	−0.431 96 (55)	0.278 96 (44)	0.230 88 (39)	2.1 (2)
C(33)	−0.425 29 (59)	0.212 91 (46)	0.271 92 (39)	2.5 (2)
C(34)	−0.434 68 (52)	0.139 76 (45)	0.240 47 (40)	2.2 (2)
C(35)	−0.448 37 (49)	0.131 73 (40)	0.169 22 (37)	1.8 (2)
C(36)	−0.453 55 (49)	0.197 99 (40)	0.128 06 (36)	1.6 (2)
C(37)	−0.598 03 (47)	0.372 05 (38)	0.059 89 (36)	1.5 (2)
C(38)	−0.659 69 (52)	0.367 55 (43)	0.101 75 (38)	2.0 (2)
C(39)	−0.760 27 (56)	0.382 35 (46)	0.070 48 (48)	2.8 (3)
C(40)	−0.800 50 (53)	0.401 72 (45)	−0.001 25 (47)	2.8 (2)
C(41)	−0.740 12 (55)	0.404 76 (44)	−0.042 03 (41)	2.5 (2)
C(42)	−0.639 10 (53)	0.390 59 (42)	−0.011 56 (39)	2.0 (2)
C(43)	−0.411 81 (46)	0.441 39 (37)	0.154 74 (35)	1.3 (2)
C(44)	−0.316 21 (50)	0.436 11 (41)	0.205 99 (38)	1.8 (2)
C(45)	−0.270 89 (50)	0.501 74 (44)	0.242 42 (38)	2.1 (2)
C(46)	−0.320 21 (51)	0.573 09 (40)	0.228 98 (37)	1.7 (2)
C(47)	−0.415 77 (51)	0.578 34 (40)	0.178 73 (37)	1.7 (2)
C(48)	−0.462 01 (48)	0.512 64 (37)	0.141 19 (34)	1.3 (2)

Table III. Positional Parameters and B_{eq} for $[PPh_4]_2[Ni(WSe_4)_2]$

atom	x	y	z	B_{eq}, Å^2
W(1)	0.093 471 (26)	−0.265 788 (20)	0.134 458 (19)	0.859 (7)
Ni	0	0	0	0.86 (3)
Se(1)	0.126 133 (71)	−0.377 875 (54)	0.023 539 (50)	1.27 (2)
Se(2)	0.142 022 (82)	−0.397 983 (59)	0.327 942 (52)	1.70 (2)
Se(3)	−0.155 490 (66)	−0.120 019 (52)	0.101 221 (50)	1.13 (2)
Se(4)	0.248 623 (68)	−0.139 789 (55)	0.076 317 (58)	1.47 (2)
P(1)	0.410 06 (16)	−0.247 94 (13)	−0.332 63 (12)	0.81 (4)
C(1)	0.640 15 (65)	0.383 59 (51)	0.244 70 (47)	0.9 (2)
C(2)	0.773 61 (68)	0.392 21 (53)	0.277 04 (51)	1.2 (2)
C(3)	0.811 88 (72)	0.498 52 (57)	0.215 34 (54)	1.4 (2)
C(4)	0.717 40 (75)	0.596 13 (54)	0.120 38 (53)	1.4 (2)
C(5)	0.585 88 (73)	0.586 49 (53)	0.088 47 (48)	1.4 (2)
C(6)	0.545 23 (67)	0.481 32 (53)	0.150 22 (50)	1.1 (2)
C(7)	0.454 34 (63)	0.224 87 (50)	0.257 89 (47)	0.9 (2)
C(8)	0.303 13 (67)	0.305 51 (52)	0.238 32 (50)	1.1 (2)
C(9)	0.197 41 (69)	0.282 81 (56)	0.187 01 (52)	1.3 (2)
C(10)	0.242 00 (74)	0.180 39 (60)	0.157 61 (53)	1.5 (2)
C(11)	0.392 41 (80)	0.101 81 (60)	0.175 33 (57)	1.7 (2)
C(12)	0.500 27 (72)	0.124 64 (55)	0.225 45 (55)	1.4 (2)
C(13)	0.507 88 (63)	0.262 21 (50)	0.462 95 (47)	0.9 (2)
C(14)	0.559 14 (75)	0.321 73 (60)	0.516 67 (53)	1.5 (2)
C(15)	0.500 16 (85)	0.325 52 (65)	0.621 21 (59)	1.9 (2)
C(16)	0.390 70 (86)	0.271 88 (64)	0.670 90 (56)	1.9 (2)
C(17)	0.338 96 (81)	0.213 43 (63)	0.617 84 (55)	1.8 (2)
C(18)	0.398 03 (71)	0.207 91 (57)	0.513 93 (50)	1.3 (2)
C(19)	0.242 60 (62)	−0.111 55 (49)	−0.369 63 (47)	0.8 (1)
C(20)	0.139 12 (69)	−0.100 31 (57)	−0.282 56 (49)	1.3 (2)
C(21)	0.020 39 (69)	0.011 10 (59)	−0.305 67 (56)	1.4 (2)
C(22)	0.003 19 (70)	0.109 84 (55)	−0.415 42 (58)	1.4 (2)
C(23)	0.101 19 (68)	0.097 58 (53)	−0.502 10 (52)	1.3 (2)
C(24)	0.221 30 (65)	−0.013 36 (51)	−0.479 17 (49)	1.0 (2)

Table IV. Selected Bond Distances (Å) and Angles (deg) in $[PPh_4]_2[Ni(Se_2)(WSe_4)]$

Distances			
W–Ni	2.703 (1)	Ni–Se(1)	2.285 (1)
W–Se(1)	2.357 (1)	Ni–Se(2)	2.295 (1)
W–Se(2)	2.356 (1)	Ni–Se(5)	2.298 (1)
W–Se(3)	2.281 (1)	Ni–Se(6)	2.301 (1)
W–Se(4)	2.288 (1)	Se(5)–Se(6)	2.328 (1)
		Se(1)···Se(2)	3.774 (1)
Angles			
Se(1)–W–Se(2)	106.44 (3)	Se(1)–Ni–Se(2)	111.01 (4)
Se(1)–W–Se(4)	109.32 (4)	Se(1)–Ni–Se(5)	92.72 (4)
Se(1)–W–Se(3)	110.23 (4)	Se(1)–Ni–Se(6)	153.31 (5)
Se(2)–W–Se(3)	110.42 (3)	Se(2)–Ni–Se(5)	156.20 (5)
Se(2)–W–Se(4)	109.06 (4)	Se(2)–Ni–Se(6)	95.57 (4)
Se(3)–W–Se(4)	111.23 (6)	Se(5)–Ni–Se(6)	60.83 (4)
Ni–Se(1)–W	71.21 (3)	Se(5)–Se(6)–Ni	59.51 (3)
Ni–Se(2)–W	71.06 (3)	Se(6)–Se(5)–Ni	59.66 (4)

Table V. Selected Bond Distances (Å) and Angles (deg) in $[PPh_4]_2[Ni(WSe_4)_2]$[a]

Distances			
W–Ni	2.866 (1)	W–Se(4)	2.347 (1)
W–Se(1)	2.277 (1)	Ni–Se(3)	2.353 (1)
W–Se(2)	2.285 (1)	Ni–Se(4)	2.347 (1)
W–Se(3)	2.350 (1)	Se(3)···Se(4)′	2.941 (1)
		Se(3)···Se(4)	3.691 (1)
Angles			
Se(1)–W–Se(2)	110.15 (3)	Se(3)–W–Se(4)	103.62 (3)
Se(1)–W–Se(3)	110.14 (3)	Se(3)–Ni–Se(4)	102.90 (3)
Se(1)–W–Se(4)	111.22 (3)	Se(3)–Ni–Se(4)′	77.10 (3)
Se(2)–W–Se(3)	110.75 (3)	Ni–Se(3)–W	75.08 (3)
Se(2)–W–Se(4)	110.81 (3)	Ni–Se(4)–W	74.88 (3)

[a] Primed atoms are related to unprimed atoms through the inversion center at Ni.

$[PPh_4]_2[Ni(WSe_4)_2]$ 7295 reflections and 277 variables) to give $R(F_o^2)$ values of 0.076 and 0.090, respectively. Prior to the final cycle, phenyl H atoms were included at calculated positions (C–H = 0.95 Å) with isotropic thermal parameters 1 Å^2 greater than the equivalent isotropic thermal parameter of the attached carbon atom. Final positional parameters of all non-hydrogen atoms are given in Tables II and III. Selected bond distances and bond angles are given in Tables IV and V. The $[Ni(Se_2)(WSe_4)]^{2-}$ and $[Ni(WSe_4)_2]^{2-}$ anions are illustrated in Figures 2 and 3, respectively.

X-Ray powder diffraction patterns of $[PPh_4]_2[Ni(WSe_4)_2]$ and $[PPh_4]_2[Pd(WSe_4)_2]$ were recorded at room temperature with Cu Kα radiation on an Enraf-Nonius Model FR 552 Guinier camera; silicon powder was the standard.

Results and Discussion

Synthesis and Spectroscopy. Müller and co-workers have prepared a series of anionic mixed-metal sulfides.[1] These M′-$(MS_4)_2^{2-}$ (M = Mo, W; M′ = Fe, Co, Ni, Pd, Pt, Zn, Cd, Hg) anions all feature two nearly tetrahedral, bidentate MS_4 units bound to a M′ center. The coordination geometry about the central metal can be tetrahedral (as in $Co(WS_4)_2^{2-}$) or square planar (as in $Ni(WS_4)_2^{2-}$), while metals that prefer octahedral coordination can complete their coordination spheres with solvent molecules (as in $[Fe(WS_4)_2(dmf)_2]^{2-}$). Among potential selenium analogues only $Zn(WSe_4)_2^{2-}$ has been reported,[20] but it is not

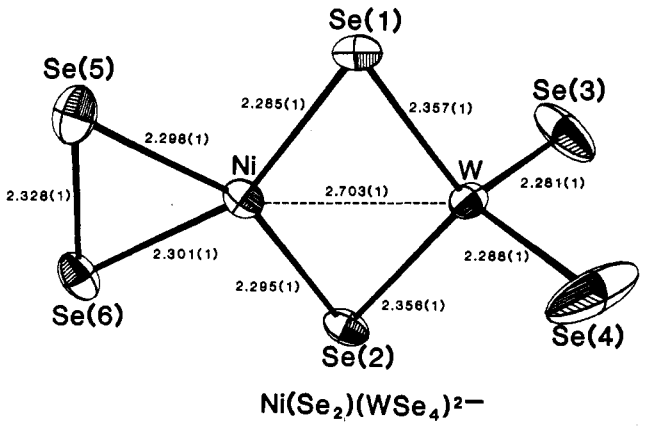

Figure 2. Structure of the $Ni(Se_2)(WSe_4)^{2-}$ ion. In this figure and in Figure 3, 50% probability ellipsoids are shown.

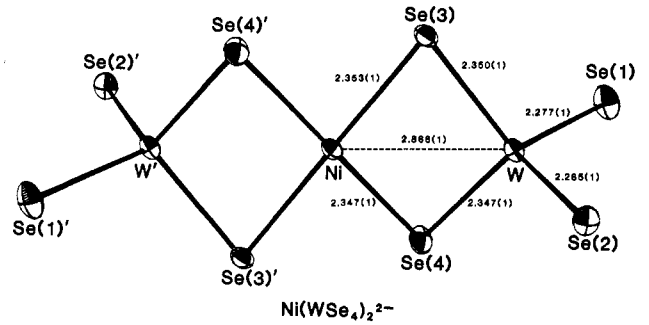

Figure 3. Structure of the $Ni(WSe_4)_2^{2-}$ ion. Atoms with primes are related by the inversion center (at Ni) to the corresponding nonprimed atoms.

especially stable and has not been characterized structurally.

Since we have recently developed new and simpler synthetic routes to the tetraselenometalates MSe_4^{2-} (M = Mo, W) and have also established ^{77}Se NMR chemical shift ranges corresponding to the different structural types of Se atoms in soluble transition-metal selenides,[15,16] we decided to investigate the reactions of the WSe_4^{2-} anion with various M^{2+} ions. Because of the known water sensitivity of the soluble transition-metal selenides, special care was taken to exclude moisture and to choose starting materials free from waters of crystallization.

In the soluble sulfides both infrared and electronic spectroscopies are of use in the characterization of products, but their usefulness in the soluble selenides is more limited. The vibrational stretches, M–Se(terminal), M–Se(bridging), M–Se(ring), and Se–Se, all appear in almost the same region of the IR spectrum (200–340 cm^{-1}) and cannot be easily distinguished from one another (see Experimental Section). All complexes synthesized here show intense bands in their absorption spectra (Figure 1). These spectra are useful for identification but not for characterization. The bands observed here are of the charge-transfer type (π(Se) → d(W)) and arise from the WSe_4 moiety. A comparison of the electronic spectra of **1**, **2**, and **3** with that of WSe_4^{2-} [1] suggests that all of the bands from WSe_4^{2-} are shifted toward higher wavelength, thereby indicating a strong interaction between the ligand (WSe_4^{2-}) and metal (Ni^{2+} or Pd^{2+}).

Fortunately, Se has an NMR-active nucleus, ^{77}Se (spin = $^1/_2$, natural abundance = 7.5%), and the use of ^{77}Se NMR spectroscopy augments analytical methods and offers structural insights for solution species.[15] Previous work in this laboratory[15,16] has established the following scale relative to Me_2Se at 0 ppm for soluble transition-metal selenides: terminal Se, $\delta > 1000$ ppm; bridging Se, $1000 \leq \delta \leq 600$ ppm; metal-bound Se (in an MSe_n ring), $1000 \leq \delta \leq 500$ ppm; ring Se (in an MSe_n ring), $\delta \leq 400$ ppm. Since ^{183}W is also an NMR-active nucleus (spin = $^1/_2$, natural abundance = 14.3%), ^{183}W satellites are expected with resonances arising from selenium atoms directly bound to tungsten. In actual practice, resonances arising from terminal selenium atoms almost never display such satellites but those arising from bridging and metal-bound selenium atoms do. With this shift scale established, ^{77}Se NMR spectroscopy has become for us an important analytical tool for soluble transition-metal selenide chemistry.

On the basis of the mixed-metal sulfide chemistry, reaction of WSe_4^{2-} with $Ni(acac)_2$ in DMF would be expected to afford $Ni(WSe_4)_2^{2-}$. However, when the ^{77}Se NMR spectrum of the reaction product was obtained, instead of the expected two resonances (from terminal and bridging Se atoms), three resonances, at δ = 1399, 855, and 608 ppm, were found. The peak at 1399 ppm comes well within the range expected for a terminal selenium atom bound to tungsten and, as is usual for such terminal resonances, shows no ^{183}W satellites. The peak at 855 ppm falls in the range seen for selenium atoms bridging two metals and shows the expected ^{183}W satellites ($^1J_{Se-W}$ = 109 Hz). The peak at 608 ppm is in the range for selenium atoms bound to the metal in a MSe_n ring (where n = 2,3,4) and, since no peaks are observed in the ring region ($\delta \leq 500$ ppm), n must be 2. The ^{183} W satellites expected if the Se_n ring were bound to tungsten are not observed for this resonance, so the Se_n ring must be bound to the nickel center. Weaker satellites for Se–Se coupling are observed here ($^2J_{Se-Se}$ = 138 Hz). IR and EDAX measurements provide no evidence for the presence of $acac^-$ or chloride (which could have acted as additional ligands not detected by ^{77}Se NMR spectroscopy). These results were thus consistent with the anion $[(Se)_2W(\mu\text{-}Se)_2Ni(Se_2)]^{2-}$; this was confirmed by the X-ray diffraction determination of the structure of the PPh_4^+ salt.

Interestingly, when a DMF solution of $[NH_4]_2[WSe_4]$ and $[PPh_4]Cl$ is added to $NiCl_2(PPh_3)_2$, the dark red crystalline product isolated shows only two ^{77}Se NMR resonances at δ = 1628 and 994 ppm. These resonances are consistent with the $Ni(WSe_4)_2^{2-}$ anion, since it contains two types of selenium: terminal (with δ = 1628 ppm) and bridging (with δ = 994 ppm). The bridging peak shows ^{183}W satellites ($^1J_{Se-W}$ = 109 Hz), and none are observed on the terminal selenium resonance. IR and EDAX spectra showed that no additional ligands were present. The formulation as $Ni(WSe_4)_2^{2-}$ was confirmed by an X-ray diffraction study of the PPh_4^+ salt.

While $[PPh_4]_2[Ni(WSe_4)_2]$ is a stable solid, in DMF solution at room temperature it slowly decomposes. From monitoring of its reaction by ^{77}Se NMR spectroscopy, we find a gradual disappearance of the two-line spectrum associated with $Ni(WSe_4)_2^{2-}$ and a concurrent appearance of the three-line spectrum of $Ni(Se_2)(WSe_4)^{2-}$. The electronic absorption (UV–vis) spectra of aliquots taken from the $Ni(Se_2)(WSe_4)^{2-}$ synthesis show that $Ni(WSe_4)_2^{2-}$ is the initial product formed within the first 10 min but is almost all converted to $Ni(Se_2)(WSe_4)^{2-}$ within 2 h. Similar spectra taken from the $Ni(WSe_4)_2^{2-}$ synthesis indicate slower formation of product, with significant amounts of uncomplexed WSe_4^{2-} still present in the reaction mixture after 20 min. Addition of acetylacetone (2,4-pentanedione) to this mixture or to the isolated $Ni(WSe_4)_2^{2-}$ product in DMF solution did not accelerate the decomposition to $Ni(Se_2)(WSe_4)^{2-}$.

Pure $[PPh_4]_2[Ni(WSe_4)_2]$ (prepared from $NiCl_2(PPh_3)_2$ and WSe_4^{2-}) was allowed to decompose by stirring in DMF under nitrogen for 24 h. The soluble product was spectroscopically identical with $[PPh_4]_2[Ni(Se_2)(WSe_4)]$ and was formed in 89% yield. The insoluble black byproduct, which could be the known solid-state compound WSe_2 (eq 1), has an X-ray powder diffraction pattern different from that of WSe_2. In fact, analysis of the black powder shows the presence of W, Se, and DMF. Because it is the product ultimately formed in each reaction of Ni and WSe_4^{2-}, the $Ni(Se_2)(WSe_4)^{2-}$ anion seems to be the more stable species. This is in marked contrast to the soluble W–Ni–S system, where attempts to synthesize a soluble mixed-metal binuclear sulfide (with a WS_2Ni^{4+} core) resulted instead in a tri-

$$Ni(WSe_4)_2^{2-} \rightarrow Ni(Se_2)(WSe_4)^{2-} + WSe_2 \qquad (1)$$

(20) Müller, A.; Ahlborn, E.; Heinsen, H.-H. *Z. Anorg. Allg. Chem.* **1971**, *386*, 102–106.

nuclear species with a $WS_2NiS_2W^{6+}$ core. These differences in stability could result from the larger size of the Se atom versus that of the S atom.

In contrast to the Ni–W–Se system, reaction of $PdCl_2(C_6H_5CN)_2$ with WSe_4^{2-} and PPh_4^+ in DMF solution affords only $[PPh_4]_2[Pd(WSe_4)_2]$. X-ray powder photography indicates that $[PPh_4]_2[Pd(WSe_4)_2]$ and $[PPh_4]_2[Ni(WSe_4)_2]$ are isostructural. As predicted for the $Pd(WSe_4)_2^{2-}$ anion, ^{77}Se NMR spectroscopy shows only one bridging (δ = 1135 ppm, $^1J_{Se-W}$ = 119 Hz) and one terminal (δ = 1673 ppm) resonance. In contrast to $Ni(WSe_4)_2^{2-}$, which decomposes to $Ni(Se_2)(WSe_4)^{2-}$, solutions of $Pd(WSe_4)_2^{2-}$ in DMF are stable under dinitrogen.

A comparison of ^{77}Se NMR resonances for these $M(WSe_4)_2^{2-}$ compounds shows a deshielding, downfield shift for M = Pd (δ = 1673 and 1135 ppm) versus that for M = Ni (δ = 1628 and 994 ppm). The shift is greatest for the bridging selenium atoms, since they are directly bound to the central metal. The larger size of Pd versus that of Ni probably allows greater orbital overlap with Se, leading to increased electron donation to the central metal ion and the observed deshielding. Interestingly, ^{77}Se NMR spectroscopy of $MoSe_4^{2-}$ (δ = 1643 ppm) and WSe_4^{2-} (δ = 1235 ppm)[16] shows a deshielding effect for Mo versus that for W. Perhaps second-row transition metals (i.e. Mo and Pd) have better orbital overlap with Se than either first- or third-row transition metals. The terminal Se resonances on the WSe_4 units in $Ni(Se_2)(WSe_4)^{2-}$, $Ni(WSe_4)_2^{2-}$, and $Pd(WSe_4)_2^{2-}$ are deshielded relative to uncomplexed WSe_4^{2-} (δ = 1399, 1628, and 1673 versus δ = 1235 ppm for WSe_4^{2-}). This is consistent with the view that tetraselenometalates are good electron-donating ligands.

Structures. The structure of the $Ni(Se_2)(WSe_4)^{2-}$ ion (Figure 2) is unique, having no analogues in the literature. It and $Ni(WSe_4)_2^{2-}$ (Figure 3) are the first mixed-metal selenide clusters to be structurally characterized. These anions are well separated from the PPh_4^+ cations in the solid state; there are no unusual cation–anion interactions. The cations show the expected geometry.[21]

The $Ni(WSe_4)_2^{2-}$ anion is analogous to $Ni(WS_4)_2^{2-}$.[22] In particular, the anion has a crystallographically imposed center of inversion, with the Ni center being square-planar and bound to two slightly distorted tetrahedral WSe_4 groups. The angle between the Ni, Se(3), Se(4), Se(3′), and Se(4′) plane and that formed by W, Se(1), and Se(2) is 89.44°. The terminal W–Se distances of 2.277 (1) and 2.285 (1) Å are longer than those of 2.314 (1) Å in the WSe_4^{2-} ion[1,17,23] but are shorter than the bridging W–Se distances of 2.349 (1) and 2.347 (1) Å. In the corresponding S analogue[22] the terminal W–S distances are 2.150 (5) and 2.151 (4) Å, while the bridging W–S distances are 2.234 (3) and 2.229 (4) Å, to be compared with the W–S distance of 2.165 Å in the WS_4^{2-} ion.[24] Note that in $Ni(WS_4)_2^{2-}$ the W–S distances are about 0.13 Å shorter than the W–Se distances in $Ni(WSe_4)_2^{2-}$. On the other hand, the $W(\mu\text{-}Se)_2Ni$ arrangement is somewhat different. In the S compound, the W–Ni distance is 2.817 (1) Å, some 0.05 Å shorter than in the Se compound (2.866 (1) Å), and the angles at S are larger (78.1 (1) vs 75.0 (1)°), while the angles at W are smaller (101.5 (1) vs 103.62 (3)°). The net result is a trans-bridge S···S distance of 3.458 (6) Å vs a Se···Se distance of 3.691 (1) Å. Presumably, these changes in geometry are dictated by the larger Se atoms, since the approximate 0.13 Å larger radius of Se compared with S is maintained.

The $Ni(Se_2)(WSe_4)^{2-}$ anion contains a square-planar Ni center bound to a slightly distorted tetrahedral WSe_4 group and a side-on Se_2 ligand. The best least-squares plane through the Ni, Se(1), Se(2), Se(5), and Se(6) atoms has an average deviation of 0.041 (1) Å. The angle between this plane and that formed by the W, Se(3), and Se(4) atoms is 89.1°. The Ni–W distance of 2.703 (1) Å is much shorter than in $Ni(WSe_4)_2^{2-}$ (2.866 (1) Å). The Se–Se distance in the Se_2 ligand is 2.328 (1) Å, which is normal for a side-on-bound Se_2 ligand (i.e.: $W_2Se_9^{2-}$, 2.340 (4) Å;[15] $W_2Se_{10}^{2-}$, 2.340 (4) Å;[15] $V_2Se_{13}^{2-}$, 2.334 (3) Å;[14] $Ir(Se_2)(dppe)_2^+$, 2.312 (3) Å;[25] $Os(Se_2)(CO)_2(PPh_3)_2$, 2.321 (1) Å[26]). As is the case with olefins bound to metals, this WSe_2 geometry can be described either in terms of σ-bonding, and hence a cyclopropane-type system, or in terms of a π-bound Se_2 ligand. The W–Se distances in $Ni(Se_2)(WSe_4)^{2-}$ differ insignificantly from those in $Ni(WSe_4)_2^{2-}$. However, the $W(\mu\text{-}Se)_2Ni$ geometry does differ. In $Ni(Se_2)(WSe_4)^{2-}$ the angles at W, Ni, and Se are 106.44 (3), 111.01 (4), and 71.14 (3)°, respectively, while the corresponding angles in $Ni(WSe_4)_2^{2-}$ are 103.62 (3), 102.90 (3), and 75.48 (3)°. The trans Se···Se distance of 3.774 (1) Å vs 3.691 (1) Å is expected from these changes and from the shortening of the W–Ni bond. The geometries about Ni are very different in the two compounds. In particular, the Ni–Se bridge distances are much shorter in $Ni(Se_2)(WSe_4)^{2-}$ (2.285 (1) Å vs 2.347 (1) and 2.353 (1) Å), presumably because there is no longer a Se atom directly trans to these Ni–Se bridges. In fact, the Se(2)–Ni–Se(5) and Se(1)–Ni–Se(6) bond angles of 153.31 (5) and 156.20 (5)° are much smaller than those of 180° required by symmetry in $Ni(WSe_4)_2^{2-}$.

Acknowledgment. This research was supported by the National Science Foundation (Grant No. CHE-8701007).

Supplementary Material Available: Complete crystallographic details (Table IS) and anisotropic thermal parameters and hydrogen atom positions for $[PPh_4]_2[Ni(Se_2)(WSe_4)]$ (Table IIS) and $[PPh_4]_2[Ni(WSe_4)_2]$ (Table IVS) (4 pages); Tables IIIS and VS of structure amplitudes (71 pages). Ordering information is given on any current masthead page.

(21) The 24 phenyl C–C distances average 1.387 (13) Å in **1**, while the 48 C–C distances average 1.388 (8) Å in **2**, where the numbers in parentheses are estimated standard deviations of a single observation. These may be compared with 0.010 and 0.009 Å, respectively, as estimated from the inverse matrices. These results suggest that standard deviations in the two structures are correctly estimated.

(22) Müller, A.; Bögge, H.; Krickemeyer, E.; Henkel, G.; Krebs, B. *Z. Naturforsch., B: Anorg. Chem., Org. Chem.* **1982**, *37B*, 1014–1019.
(23) Müller, A.; Krebs, B.; Beyer, H. *Z. Naturforsch., B: Anorg. Chem., Org. Chem., Biochem., Biophys., Biol.* **1968**, *23B*, 1537–1538.
(24) Sasvári, K. *Acta Crystallogr.* **1963**, *16*, 719–724.
(25) Ginsberg, A. P.; Lindsell, W. E.; Sprinkle, C. R.; West, K. W.; Cohen, R. L. *Inorg. Chem.* **1982**, *21*, 3666–3681.
(26) Farrar, D. H.; Grundy, K. R.; Payne, N. C.; Roper, W. R.; Walker, A. *J. Am. Chem. Soc.* **1979**, *101*, 6577–6582.